

Conjugated Microporous Polymers as Molecular Sensing Devices: Microporous Architecture Enables Rapid Response and Enhances Sensitivity in Fluorescence-On and Fluorescence-Off Sensing

Xiaoming Liu,[†] Yanhong Xu, and Donglin Jiang*

Department of Materials Molecular Science, Institute for Molecular Science, National Institutes of Natural Sciences, 5-1 Higashiyama, Myodaiji, Okazaki 444-8787, Japan

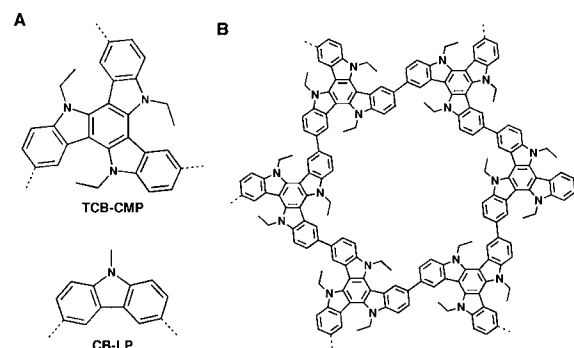
S Supporting Information

ABSTRACT: Conjugated polymers are attractive materials for the detection of chemicals because of their remarkable π -conjugation and photoluminescence properties. In this article, we report a new strategy for the construction of molecular detection systems with conjugated microporous polymers (CMPs). The condensation of a carbazole derivative, TCB, leads to the synthesis of a conjugated microporous polymer (TCB-CMP) that exhibits blue luminescence and possesses a large surface area. Compared with a linear polymer analogue, TCB-CMP showed enhanced detection sensitivity and allowed for the rapid detection of arenes upon exposure to their vapors. TCB-CMP displayed prominent fluorescence enhancement in the presence of electron-rich arene vapors and drastic fluorescence quenching in the presence of electron-deficient arene vapors, and it could be reused without a loss of sensitivity and responsiveness. These characteristics are attributed to the microporous conjugated network of the material. Specifically, the micropores absorb arene molecules into the confined space of the polymer, the skeleton possesses a large surface area and provides a broad interface for arenes, and the network architecture facilitates exciton migration over the framework. These structural features function cooperatively, enhancing the signaling activity of TCB-CMP in fluorescence-on and fluorescence-off detection.

Conjugated polymers are fascinating materials with π -conjugation and light-emitting properties that allow for the detection of various chemicals.^{1,2} Specific sites that interact with target compounds can be introduced into conjugated chains to enhance the interaction interface and improve the signaling activity. Conjugated microporous polymers (CMPs) are a class of porous polymers with a conjugated network structure.^{3–6} In this context, CMPs are attractive candidates because they possess large surface areas and provide a broad interface for analyte interaction. Nevertheless, until now, CMPs that enable the detection of chemicals have not been synthesized. Herein we report the first example of a chemosensing CMP and highlight the cooperative nature of its structure features, which allow the material to achieve rapid response times and dramatically enhanced detection sensitivities.

We synthesized a diindolocarbazole monomer for the construction of TCB-CMP, a carbazole-based CMP (Chart 1A), through the Yamamoto reaction [see the Supporting

Chart 1. Schematic Representations of (A) the Carbazole-Based CMP (TCB-CMP) and the Linear Polymer Analogue CB-LP and (B) the Elementary Pore Skeleton of TCB-CMP Containing TCB Units



Information (SI)]. Polymeric carbazole derivatives have been developed as fluorescent platforms for detecting explosives.² As a control, we also prepared CB-LP, a linear conjugated analogue with a polycarbazole chain (Chart 1A). TCB-CMP was characterized by Fourier transform IR spectroscopy, elemental analysis, and ¹³C cross-polarization/magic-angle-spinning (CP/MAS) NMR spectroscopy (Figures S1 and S2 in the SI). Field-emission scanning electron microscopy (FE-SEM) images showed that TCB-CMP adopted a flake morphology with a size of 200–500 nm. High-resolution transmission electron microscopy (HR-TEM) revealed the presence of a porous texture, and pore sizes less than 2 nm were observed. One of the most significant features of this novel material is its homogeneous pore distribution (Figure 1B). X-ray diffraction measurements did not produce any signals, indicating that TCB-CMP is an amorphous polymer (Figure S3).

TCB-CMP exhibited type-I N₂ sorption isotherms, which are indicative of a microporous structure (Figure 2A). The Brunauer–Emmett–Teller (BET) surface area and pore volume were calculated to be 1280 m² g⁻¹ and 0.923 cm³

Received: January 10, 2012

Published: May 16, 2012

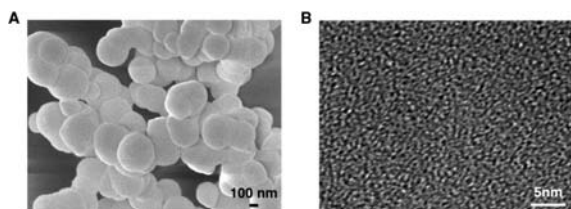


Figure 1. (A) FE-SEM and (B) HR-TEM images of TCB-CMP.

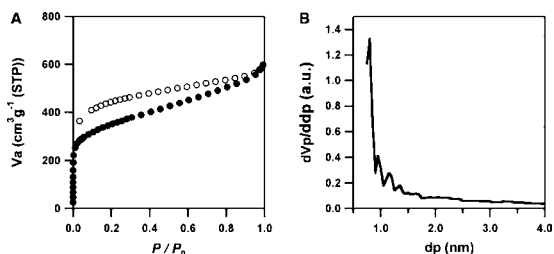


Figure 2. (A) N_2 sorption isotherm measured at 77 K and (B) pore width distribution profile of TCB-CMP.

g^{-1} , respectively. The micropore distribution pattern was determined using the Saito–Flory method. The pore size was 0.8–1.5 nm (Figure 2B), which is reasonable considering the presence of a cross-linked network and the elementary pore skeleton of TCB-CMP (Chart 1B). Therefore, the Yamamoto reaction can be used to synthesize high-surface-area microporous polymers with pores that are open and accessible to external molecules.

TCB-CMP exhibited an absorption band at 384 nm (Figure 3A, dotted red curve), which is red-shifted from that of TCB by

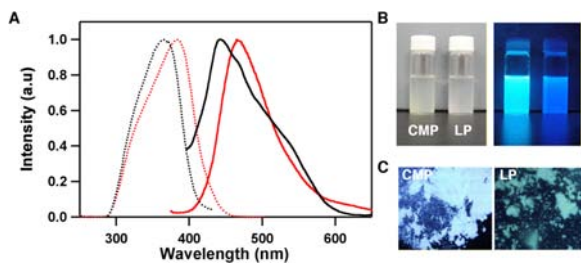


Figure 3. (A) Electronic absorption (dotted curves) and fluorescence spectra (solid curves) of TCB-CMP (red) and CB-LP (black) powders. (B) Images of TCB-CMP and CB-LP (left) in PEG and (right) under a UV lamp. (C) Fluorescence microscopy images of solid samples of TCB-CMP and CB-LP.

20 nm. TCB-CMP displayed blue luminescence (Figure 3B,C), and an emission band was observed at 468 nm with a quantum yield of 10% (Figure 3A, solid red curve) upon excitation at 368 nm. In contrast, CB-LP displayed an absorption band at 363 nm (Figure 3A, dotted black curve) and emitted luminescence at 445 nm with a quantum yield of 0.6% (Figure 3A, solid black curve; Figure 3B,C). Because the CMP network allows for extended electronic conjugation, we investigated the fluorescence depolarization profile of TCB-CMP, which reflects the occurrence of photochemical events in microporous networks. The suppression of Brownian motion in a viscous medium results in fluorescence depolarization, which occurs predominantly by exciton migration along the conjugated chain. Here, the degree of fluorescence depolarization (p) is defined as $p = (I_{\parallel} - GI_{\perp}) / (I_{\parallel} + GI_{\perp})$, where I_{\parallel} and I_{\perp} are the fluorescence

intensities of the parallel and perpendicular components relative to the polarity of the excitation light, respectively, and G is an instrumental correction factor. Excitation at the absorption maximum of viscous of TCB-CMP in poly(ethylene glycol) (PEG) at 25 °C (images are shown in Figure 3B) led to fluorescence depolarization, and the value of p was only 0.0018. In contrast, the linear polymer CB-LP exhibited a higher p value of 0.062. Therefore, the CMP architecture was significantly different from a linear chain structure, facilitating exciton migration over the three-dimensional network.

Sensing experiments were conducted by exposing thin-layer samples of TCB-CMP to arene vapors for specific periods of time at 25 °C and then performing fluorescence spectroscopy (Figure S4A–H). Prior to exposure to arene vapor, no pretreatment was performed to remove air from the micropores of the material. The results showed that TCB-CMP is quite sensitive to arenes. For example, upon exposure to the vapor of 2,4-dinitrotoluene (DNT) for only 20 s, the fluorescence of TCB-CMP was significantly quenched (Figure 4A, red circles),

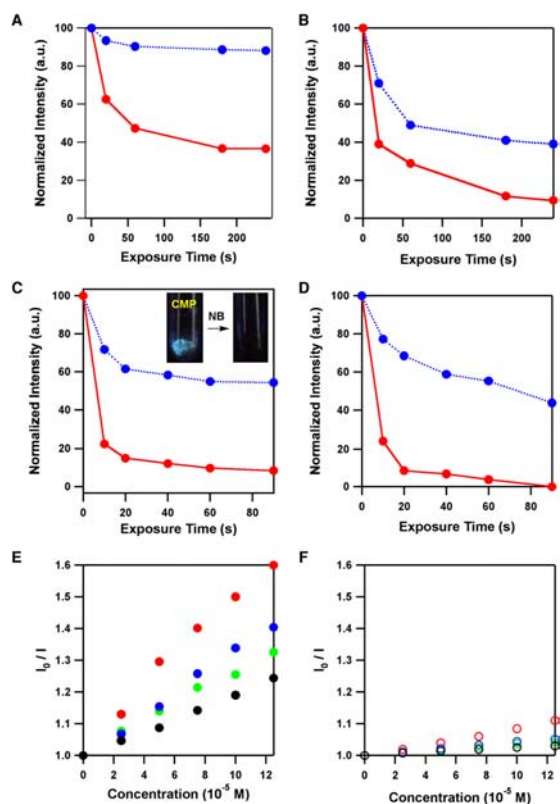


Figure 4. Loss of fluorescence intensity of TCB-CMP (red ●) and CB-LP (blue ●) at 25 °C upon exposure to vapors of (A) DNT, (B) NT, (C) NB, and (D) BQ. (E, F) Stern–Volmer plots of (E) TCB-CMP and (F) CB-LP upon titration with various arenes (red, DNT; blue, NB; green, BQ; black, NT) in acetonitrile. Inset in (C): luminescence images of TCB-CMP in the presence and absence of NB under a hand-held UV lamp.

and only 60% of the intensity of pristine TCB-CMP remained. As the exposure time was prolonged, further quenching was observed, and the fluorescence gradually saturated at 40% of the original intensity. In view of the fact that DNT has a quite low vapor pressure, it is interesting that TCB-CMP shows a high sensitivity to DNT. Under identical conditions, the linear analogue CB-LP showed a low degree of quenching, and the maximum quenching percentage was only 10% (Figure 4A, blue

circles). Interestingly, the fluorescence-off sensing behavior was not specific to DNT but was also applicable to other electron-deficient arenes. TCB-CMP exhibited an enhanced response to 2-nitrotoluene (NT), and 60% of the fluorescence was quenched upon exposure to NT for 20 s (Figure 4B, red circles). In contrast, the fluorescence quenching was only 30% for CB-LP (Figure 4B, blue circles). Notably, 80% of the fluorescence of TCB-CMP was quenched upon exposure to nitrobenzene (NB) for only 10 s (Figure 4C, red circles and inset). Significant fluorescence quenching was also observed for 1,4-benzoquinone (BQ). In particular, 10 s of exposure produced an 80% loss of fluorescence (Figure 4D, red circles). After only 90 s of exposure, the fluorescence of TCB-CMP was completely quenched. In contrast, CB-LP exhibited a low degree of quenching, and longer exposure times were required to quench the fluorescence (Figure 4D, blue circles). These results indicate that the microporous architecture facilitates the sensing process and improves the response to the arenes.

To gain insight into the fluorescence quenching process, TCB-CMP was titrated with various arenes in acetonitrile at 25 °C. As shown in Figure 4E, the fluorescence intensity of TCB-CMP decreased linearly with an increase in the arene concentration because of photoinduced electron transfer from TCB-CMP to the arene. The Stern–Volmer constant, K_{SV} , was $1.9 \times 10^3 \text{ M}^{-1}$ for NT and increased to 2.6×10^3 , 3.1×10^3 , and $5.9 \times 10^3 \text{ M}^{-1}$ for BQ, NB, and DNT, respectively. This general trend is in good agreement with the trend in reduction potentials of nitro-substituted arenes. However, the observed trend for the degree of fluorescence quenching by arene vapors was different from that for the K_{sv} values. Because the sensing of arene vapors depends on two analyte characteristics, namely, the reduction potential and the vapor pressure, this observation could be attributed to the differences in the saturated vapor pressures of the studied arenes (Table S1 in the SI). Arenes with a large K_{sv} and a high vapor pressure can be detected with high sensitivity. Alternatively, the linear analogue CB-LP gave low K_{SV} values of only 2.3×10^2 , 3.3×10^2 , 4.1×10^2 , and $8.8 \times 10^2 \text{ M}^{-1}$ for NT, BQ, NB, and DNT, respectively. Thus, TCB-CMP allows for efficient electron transfer to electron-deficient arenes, which enhances the detection sensitivity. These results indicate that the function of the CMP architecture is multifold: the extended π -conjugation network allows exciton migration, the high-surface-area skeleton provides a broad interface for electron transfer, and the micropores hold the arene molecules in a confined space. These features cooperate to facilitate the signaling process and improve the response.

As in the case of electron-deficient arenes, the microporous skeleton of TCB-CMP is accessible to electron-rich arenes. Interestingly, however, in contrast to electron-deficient arenes, which induced fluorescence quenching, the presence of electron-rich arenes enhanced the TCB-CMP fluorescence intensity (Figure S4I–P). For example, upon exposure to chlorobenzene vapor for 20 s, the fluorescence intensity of TCB-CMP increased by 78% (Figure 5A, red circles), which was significantly greater than the increase for CB-LP (18%, blue circles). Similarly, mesitylene vapor caused a 79% enhancement in the fluorescence intensity of TCB-CMP (Figure 5B, red circles). The quick response and rapid saturation of the fluorescence intensity indicated that the porous network is extremely sensitive to these arenes. Remarkably, upon exposure to benzene vapor for 20 s, the fluorescence intensity of TCB-CMP nearly doubled (Figure 5C, red circles). The most explicit enhancement was observed for toluene vapor, which induced a

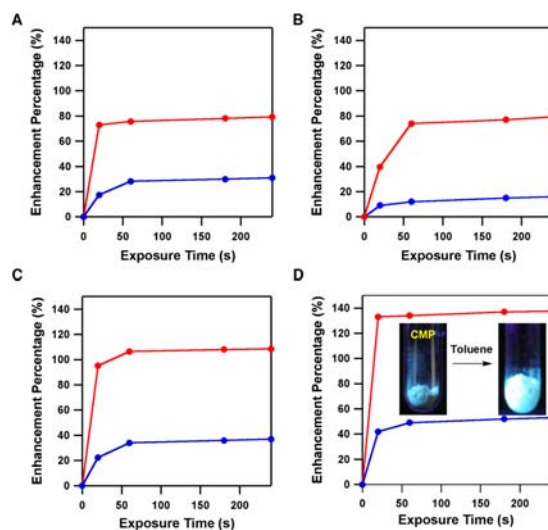


Figure 5. Fluorescence enhancement of TCB-CMP (red ●) and CB-LP (blue ●) upon exposure to vapors of (A) chlorobenzene, (B) mesitylene, (C) benzene, and (D) toluene. Inset in (D): luminescence images of CMP in the presence and absence of toluene under a hand-held UV lamp.

fluorescence intensity increase of 135% after only 20 s of exposure (Figure 5D, red circles and inset). The observed fluorescence enhancement was clearly correlated with the electron-donating properties and vapor pressure of the arenes (Table S1). Large gaps between TCB-CMP and CB-LP (Figure 5A–D, blue circles) were observed for all of the tested arenes. Therefore, microporous conjugated skeletons are superior to linear chains in the fluorescence-on sensing of arenes. CMPs possess multiple functions, and their structural features cooperate to enhance the detection sensitivity.

TCB-CMP can be reused in both the fluorescence-on and fluorescence-off sensing of arenes. For example, upon exposure to NB vapor for 20 s, TCB-CMP exhibited the same degree of fluorescence quenching after each cycle, and the fluorescence intensity recovered to a similar level when the NB vapor was removed. Therefore, TCB-CMP maintains high sensitivity and a rapid response time (Figure 6A). Moreover, TCB-CMP

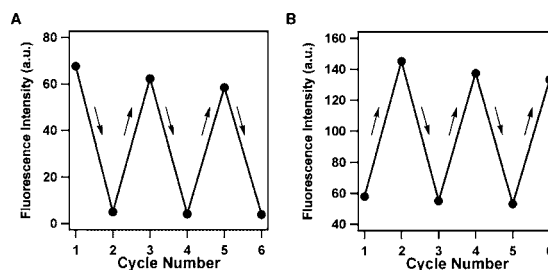


Figure 6. Cycling tests of TCB-CMP upon exposure to vapors of (A) NB and (B) toluene.

exhibited a remarkable enhancement in fluorescence upon exposure to toluene vapor for 20 s, even after reuse (Figure 6B). Similar increases in the degree of fluorescence intensity were observed during each cycling test. Because of the interweaving nature of the network skeleton, TCB-CMP can be used repetitively, and a significant deterioration in the sensitivity and response does not occur.

The top of the valence band and the bottom of the conduction band of TCB-CMP lie at approximately -5.2 and -2.38 eV, respectively, as estimated from cyclic voltammetry and absorption spectroscopy. The bottom of the conduction band of TCB-CMP is higher than the lowest unoccupied molecular orbitals (LUMOs) of electron-deficient arenes, which drives electron transfer and causes fluorescence quenching, as observed for other conjugated polymers (Figure S5A).^{1,7} Alternatively, when an electron-rich arene possesses a LUMO that is higher than the conduction band of TCB-CMP, the electrons of the arene flow to the conduction band of TCB-CMP, which enhances the fluorescence intensity (Figure S5B).^{1,7} Differences in the fluorescence-on and -off mechanisms of TCB-CMP allow for the clear visual discrimination of electron-rich and electron-deficient arenes, and the fluorescence can be simply determined with a hand-held UV lamp.

In summary, through the construction of a conjugated microporous network, we have developed a highly luminescent CMP that can be used to sense chemicals. TCB-CMP is unique in that it discriminates between electron-rich and electron-deficient arenes and provides opposite output with fluorescence-on and fluorescence-off characteristics. Remarkably, the structural features of CMPs work cooperatively in the process of sensing. Specifically, the conjugated network facilitates exciton migration over the skeleton, the large surface area of the skeleton broadens the interface between the CMP and the arene, and the micropores confine the arene molecules. These characteristics are inherent and endow CMPs with rapid response times and high sensitivity. The CMP architecture provides a unique platform for the design of de novo chemosensing systems, which can be difficult to achieve with conventional conjugated polymers. Considering the structure versatility and design flexibility of the conjugated skeletons and nanopores of CMPs, we anticipate the emergence of a fertile and exciting field focused on the development of highly sensitive sensors and sensor arrays based on luminescent CMPs.

■ ASSOCIATED CONTENT

Supporting Information

Detailed experimental procedures, characterizations, and spectral profiles. This material is available free of charge via the Internet at <http://pubs.acs.org>.

■ AUTHOR INFORMATION

Corresponding Author

jiang@ims.ac.jp

Present Address

[†]College of Chemistry, Jilin University, Changchun 130023, China (X.L.).

Notes

The authors declare no competing financial interest.

■ ACKNOWLEDGMENTS

We are grateful for the financial support of PRESTO, JST. This work was supported by a Grant-in-Aid for Scientific Research (A) (24245030) from MEXT, Japan, and partially by the NSFC (Grant 21128001).

■ REFERENCES

- (1) (a) Toal, S. J.; Trogler, W. C. *J. Mater. Chem.* **2006**, *16*, 2871. (b) Rose, A.; Zhu, Z.; Madigan, C. F.; Swager, T. M.; Bulovic, V.

Nature **2005**, *434*, 876. (c) McQuade, D. T.; Pullen, A. E.; Swager, T. M. *Chem. Rev.* **2000**, *100*, 2537. (d) Thomas, S. W.; Joly, G. D.; Swager, T. M. *Chem. Rev.* **2007**, *107*, 1339. (e) Yang, J.-S.; Swager, T. M. *J. Am. Chem. Soc.* **1998**, *120*, 11864. (f) Yang, J.-S.; Swager, T. M. *J. Am. Chem. Soc.* **1998**, *120*, 5321. (g) Swager, T. M. *Acc. Chem. Res.* **1998**, *31*, 201.

(2) (a) Naddo, T.; Che, Y.; Zhang, W.; Balakrishnan, K.; Yang, X.; Yen, M.; Zhao, J.; Moore, J. S.; Zang, L. *J. Am. Chem. Soc.* **2007**, *129*, 6978. (b) Che, Y.; Gross, D. E.; Huang, H.; Yang, D.; Yang, X.; Discekici, E.; Xue, Z.; Zhao, H.; Moore, J. S.; Zang, L. *J. Am. Chem. Soc.* **2012**, *134*, 4978. (c) Lubczyk, D.; Grill, M.; Baumgarten, M.; Waldvogel, S. R.; Müllen, K. *ChemPlusChem* **2012**, *77*, 102. (d) Nie, H.; Zhao, Y.; Zhang, M.; Ma, Y.; Baumgarten, M.; Müllen, K. *Chem. Commun.* **2011**, *47*, 1234. (e) Nie, H.; Sun, G.; Zhang, M.; Baumgarten, M.; Müllen, K. *J. Mater. Chem.* **2012**, *22*, 2129. (f) Dierschke, F.; Grimsdale, A. C.; Müllen, K. *Synthesis* **2003**, 2470. (g) Schmaltz, B.; Rouhanipour, A.; Räder, H. J.; Pisula, W.; Müllen, K. *Angew. Chem., Int. Ed.* **2009**, *48*, 720. (h) Dierschke, F.; Grimsdale, A. C.; Müllen, K. *Makromol. Chem. Phys.* **2004**, *205*, 1147. (i) Gao, P.; Cho, D.; Yang, X.; Enkelmann, V.; Baumgarten, M.; Müllen, K. *Chem.—Eur. J.* **2010**, *16*, 5119. (j) Li, J.; Dierschke, F.; Wu, J.; Grimsdale, A. C.; Müllen, K. *J. Mater. Chem.* **2006**, *16*, 96.

(3) (a) Cooper, A. I. *Adv. Mater.* **2009**, *21*, 1291. (b) Thomas, A.; Kuhn, P.; Weber, J.; Titirici, M. M.; Antonietti, M. *Macromol. Rapid Commun.* **2009**, *30*, 221.

(4) (a) Jiang, J. X.; Su, F.; Trewin, A.; Wood, C. D.; Campbell, N. L.; Niu, H.; Dickinson, C.; Ganin, A. Y.; Rosseinsky, M. J.; Khimyak, Y. Z.; Cooper, A. I. *Angew. Chem., Int. Ed.* **2007**, *46*, 8574. (b) Jiang, J. X.; Su, F.; Trewin, A.; Wood, C. D.; Niu, H.; Jones, J. T. A.; Khimyak, Y. Z.; Cooper, A. I. *J. Am. Chem. Soc.* **2008**, *130*, 7710. (c) Jiang, J. X.; Su, F. B.; Niu, H. J.; Wood, C. D.; Campbell, N. L.; Khimyak, Y. Z.; Cooper, A. I. *Chem. Commun.* **2008**, 486. (d) Stöckel, E.; Wu, X. F.; Trewin, A.; Wood, C. D.; Clowes, R.; Campbell, N. L.; Jones, J. T. A.; Khimyak, Y. Z.; Adams, D. J.; Cooper, A. I. *Chem. Commun.* **2009**, 212. (e) Jones, J. T. A.; Holden, D.; Mitra, T.; Hasell, T.; Adams, D. J.; Jelfs, K. E.; Trewin, A.; Willock, D. J.; Day, G. M.; Bacsa, J.; Steiner, A.; Cooper, A. I. *Angew. Chem., Int. Ed.* **2011**, *50*, 749. (f) Dawson, R.; Laybourn, A.; Clowes, R.; Khimyak, Y. Z.; Adams, D. J.; Cooper, A. I. *Macromolecules* **2009**, *42*, 8809. (g) Hasell, T.; Wood, C. D.; Clowes, R.; Jones, J. T. A.; Khimyak, Y. Z.; Adams, D. J.; Cooper, A. I. *Chem. Mater.* **2010**, *22*, 557. (h) Jiang, J. X.; Wang, C.; Laybourn, A.; Hasell, T.; Clowes, R.; Khimyak, Y. Z.; Xiao, J. L.; Higgins, S. J.; Adams, D. J.; Cooper, A. I. *Angew. Chem., Int. Ed.* **2011**, *50*, 1072. (i) Jiang, J.-X.; Trewin, A.; Adams, D. J.; Cooper, A. I. *Chem. Sci.* **2011**, *2*, 1777.

(5) (a) Bojdy, M. J.; Wohlgemuth, S. A.; Thomas, A.; Antonietti, M. *Macromolecules* **2010**, *43*, 6639. (b) Schmidt, J.; Weber, J.; Epping, J. D.; Antonietti, M.; Thomas, A. *Adv. Mater.* **2009**, *21*, 702. (c) Wang, X. C.; Maeda, K.; Thomas, A.; Takanebe, K.; Xin, G.; Carlsson, J. M.; Domen, K.; Antonietti, M. *Nat. Mater.* **2009**, *8*, 76. (d) Palkovits, R.; Antonietti, M.; Kuhn, P.; Thomas, A.; Schüth, F. *Angew. Chem., Int. Ed.* **2009**, *48*, 6909. (e) Wang, X. C.; Chen, X. F.; Thomas, A.; Fu, X. Z.; Antonietti, M. *Adv. Mater.* **2009**, *21*, 1609.

(6) (a) Chen, L.; Yang, Y.; Jiang, D. *J. Am. Chem. Soc.* **2010**, *132*, 9138. (b) Chen, L.; Yang, Y.; Guo, Z.; Jiang, D. *Adv. Mater.* **2011**, *23*, 3149. (c) Chen, L.; Honsho, Y.; Seki, S.; Jiang, D. *J. Am. Chem. Soc.* **2010**, *132*, 6742. (d) Kou, Y.; Xu, Y.; Guo, Z.; Jiang, D. *Angew. Chem., Int. Ed.* **2011**, *50*, 8753. (e) Xu, Y.; Chen, L.; Guo, Z.; Nagai, A.; Jiang, D. *J. Am. Chem. Soc.* **2011**, *133*, 17622.

(7) Pramanik, S.; Zheng, C.; Zhang, X.; Emge, T. J.; Li, J. *J. Am. Chem. Soc.* **2011**, *133*, 4153.